Cytochrome c - silver nanoparticle interactions: Spectroscopy, thermodynamic and enzymatic activity studies

Wei Liu, David Berge-Lefranc, Florence Chaspoul, Vera I Slaveykova

Cytochrome c - silver nanoparticle interactions: Spectroscopy, thermodynamic and enzymatic activity studies

Wei Liu , David Berge-Lefranc , Florence Chaspoul , Vera I. Slaveykova

A B S T R A C T

Cytochrome *c*, an iron containing metalloprotein in the mitochondria of the cells with an oxide/redox property, plays key role in the cell apoptotic pathway. In this study, the interaction of silver nanoparticles (AgNPs) with cytochrome *c* (Cyt *c*) was investigated by using a combination of spectroscopic, imaging and thermodynamic techniques, including dynamic light scattering (DLS), ultraviolet–visible (UV–vis) spectroscopy, transmission electron microscopy (TEM), fluorescence spectroscopy, near and far circular dichroism (CD) spectroscopy, and isothermal titration calorimetry (ITC). DLS and UV–vis analysis evidenced the formation of surface complexes of Cyt *c* on AgNPs. The saturation of surface coverage of AgNPs was observed at 4.36 Cyt *c* molecules per nm^2 of AgNPs. The surface complexation resulted in a promotion of the Ag dissolution overtime. The negative sign of enthalpic (ΔH) contribution suggested that electrostatic forces are indicative forces in the interaction between protein and AgNPs. Moreover, the fluorescence spectra revealed that the conformation of protein was altered around tryptophan (Trp) and tyrosine (Tyr) residues indicating the alteration of the tertiary structure of Cyt *c*. CD analysis evidenced that the secondary structure of Cyt *c* was modified under AgNPs-Cyt c interactions and the binding of Cyt *c* onto AgNPs resulted in remarkable structural perturbation around the active site heme, which in turn alter the protein enzymatic activity. The results of the present study contributed to a deeper insight on the mechanisms of interaction between NPs and biomacromolecules and could help establish the *in vivo* fate of AgNPs on cellular redox homeostasis.

1. Introduction

Manufactured nanoparticles (NPs) have attracted extensive attention in creating novel analytical tools for medicinal sciences [1,2]. Silver (Ag) NPs, in particular, are one of the most extensively studied and explored nanostructures derived from nanotechnology, thanks to their specific chemical, biological, and physical properties [3,4]. The introduction of nanoparticles into living systems necessarily involves the possibility of interactions between biomolecules and employed nanostructure, therefore the understanding of these interaction is an important aspect for their safe biological applications and risk assessment.

Cyt *c* is a globular protein (Mol. Wt. 12.4 KDa, P*I* 10.0) of ~100 amino acid residues that exhibits exceptional functional versatility. While it is not only an electron carrier in mitochondrial respiratory chain between Cyt *c* reductase and Cyt *c* oxidase complexes, but also is a main initiator of intrinsic apoptotic pathways and a redox sensor in the cytosol after release from mitochondria [5,6]. Under pro-apoptotic conditions, however, Cyt *c* gains peroxidase activity toward cardiolipin, and it translocates into the cytosol to engage in the intrinsic apoptotic pathway [7]. Cyt *c* contains four alpha helixes but not beta sheets. It has also a non-protein prosthetic group called heme that can be probed spectroscopically and via peroxidase activity [8]. This peroxidase activity, involving the use of H_2O_2, has attracted considerable attention due to bioanalytic properties for applications in biosensing, immunoassays, food industry, bioremediation, etc. [9–13]. Therefore, Cyt *c* can serve as an excellent model protein to quantitatively assess local perturbations resulting from protein-support interactions that depend on nanoscale size and surface curvature.

NPs can enter the mitochondria and may induce the conformational changes to Cyt *c* and activate the apoptotic pathways [14]. This induction of conformational change in Cyt *c* can be considered as a cytotoxic effect of NPs. Cyt *c* interactions with several nanoscale materials, including gold NPs [15–18], Zinc oxide NPs [19,20], and mesoporous silicates NPs [21–23] were studied. These studies evidenced that

existence of the relationship between the properties of the adsorbed Cyt *c* and the size [16,17,22], coating [24] and the chemistry [15,18] of the NPs. Nonetheless, no detailed characterisation and quantitative information is available concerning the influence of the nanoscale particles on the structure and function of Cyt *c*. Regarding to silver NPs, only one study focuses on the aggregation behaviour of Cyt *c* with AgNPs [25]. This study indicated that the aggregation of Cyt c-AgNPs increases with decreasing pH, increasing temperature and ionic strength due to the reduction in the thickness of electrostatic double layer on the surface of Cyt c-AgNP.

Our previous work evidenced that AgNPs can induce the conformation changes in catalase and superoxide dismutase, and depending on the protein structure, different degrees of enzymatic activity modulation was observed [26]. In addition, the protein-AgNPs complexation can cause the dissolution AgNPs, and the Ag(I) released by AgNPs can substitute for the cuproenzyme's metal cofactor, leading to a decrease in its enzymatic activity [27]. Moreover, the link between AgNPs stability, the protein conformation change, and protein function was also reported in other studies by studying the firefly luciferase [28] and azurin [29,30].

On this background, we focus in this study on Cyt *c* due to their important biological functions. Thus, the overall aim of this study is to better understand the mechanism of interaction of Cyt *c* with AgNPs, considering (i) the impact of the protein on AgNPs stability and (ii) the effect of AgNPs on protein conformation changes and function. For this end, a multimethod approach combining dynamic light scattering (DLS), transmission electron microscopy (TEM), UV–visible spectrophotometry, circular dichroism (CD) spectroscopy, and isothermal titration calorimetry (ITC) was employed to explore the behaviour of AgNPs (surface complexation, aggregation, dissolution) and the related consequences for the protein (conformation change, binding force).

2. Materiel and methods

2.1. Silver nanoparticles and proteins

Citrate-coated spherical AgNPs of 20 nm (BioPure), provided at 1.01 mg Ag mL^{-1} (2×10^{13} NP mL^{-1}) in 2 mM citrate, were purchased from Nanocomposix Eu. The characteristics of the AgNPs in the stock suspension as provided by the manufacturer can be found in Fig. S1.

Cyt *c* from bovine heart (EC 232-700-9) was purchased from Sigma-Aldrich in lyophilized forms. The powder was resuspended in 10 mM HEPES (4-(2-hydroxyethyl)-1-piperazine ethane sulfonic acid buffer. The concentration of Cyt *c* was determined measuring the absorbance at 410 nm, with $\varepsilon = 1.06 \times 10^5$ cm^{-1} M^{-1} [31].

2.2. Preparation of AgNPs suspension and AgNP - protein mixtures

The preparation and storage condition of AgNPs suspensions were described in detail in our previous study [26]. Briefly, a 10 mM HEPES, 2 mM sodium citrate buffer (pH 7.4), referred to as HEPES-citrate, was chosen to maintain the monodispersity of AgNPs [32]. AgNPs suspensions was vortexed for 45 s before use. Incubations of AgNPs with proteins (200 µl) in 1.5 ml polypropylene tubes were carried out in the dark at controlled mixing conditions (300 rpm) and temperature (25 °C) (Comfort® thermomixer, Eppendorf).

2.3. Determination of polydispersity and hydrodynamic diameter by dynamic light scattering

DLS is used for determining the Z-average hydrodynamic diameters, distributions and polydispersity of AgNPs in the absence and presence of proteins using NanoZS (Malvern Instruments Inc, UK). For the AgNPs-Cyt c interaction study experiments, the selected concentrations were 20 µM for protein and NPs to keeping a 1:1 M ratio.

2.4. UV–visible spectroscopy

UV–vis absorption spectra were recorded at room temperature with a Lambda 365UV/Visible spectrophotometer (PerkinElmer, Waltham, MA, USA). The Surface Plasmon Resonance (SPR) of AgNP peak was observed from 280 to 700 nm. The interactions of AgNP - protein was studied in mixtures containing AgNPs and Cyt *c* of 20 µM.

2.5. Fluorescence spectroscopy

Fluorescence spectroscopy studies were carried out on a spectrofluorometer (PerkinElmer Model F-4500, Waltham, MA, USA) with a 150 W xenon lamp and a 5 nm slit. For these studies, a 1 cm quartz cell was used. The fluorescence spectra of Cyt *c* treated by AgNPs were recorded in the range from 290 to 400 nm upon excitation at 280 nm. The Cyt *c* concentration remained constant at 20 µM, and the AgNPs concentrations were varied from 10 to 60 µM. The fluorescence intensities *(I)* were measured at the emission wavelength λ_{max}^{em}, and the results then compared with the initial fluorescence of individual proteins (I_0). Data were plotted with the Stern-Volmer representation: $I_0/I = f$[NPs].

2.6. Circular dichroism analysis (CD)

CD spectra were collected on a J-810 spectropolarimeter (Jasco® France, Lisses) fitted with a thermostatically controlled cell holder. An average of three scans in the far UV from 200 to 440 nm and in the near UV from 380 to 450 nm was collected at 25 °C in a 1 mm cell. The Cyt *c* concentrations were kept constant at 20 and 100 µM for far and near UV range, respectively. The AgNPs concentrations were at 20 and 100 µM and the AgNP/protein mole ratio of 1:1. The resulting CD spectra were corrected with the related controls, normalized based on protein concentration and then expressed in $\Delta\varepsilon$ (M^{-1} cm^{-1}).

2.7. Transmission electron microscopy (TEM)

The size and morphology of AgNPs in suspension and AgNP-Cyt c mixtures at a molar ratio of 1:1 were studied at t0 and 24h of incubation by TEM (Tecnai™ G2 Sphera, FEI company, USA) operation at 200 kV. The carbon-coated copper grid was immersed in the AgNP system solution for 10 s and then dried at room temperature. The different sets of images were analyzed using ImageJ software (Media Cybernetics, Bethesda, MD, USA) for the estimation of AgNP size distributions.

2.8. Isothermal titration calorimetry

Isothermal titration calorimetry (ITC) experiments were performed on an ITC200 instrument (GE Healthcare, Microcal, Northampton, USA) at 25 °C. Forty microlitres of Cyt *c* solutions 20 µM was added by syringe to the sample cell containing AgNPs solutions at 15 µM. The Cyt *c* solution was added sequentially after an initial injection of 0.1 µL by adding 19 injections of 0.5 µL. The experiments were repeated three times and the signal was corrected by subtracting blank titration in order to remove dilution and mixing enthalpies. In order to improve the precision of the adsorption process at very low coverage, the concentrations were increased to 80 µM for CytC and 225 µM for AgNPs and the volume increased at 2 µL, all other parameters remain constant.

2.9. Peroxidase activity of Cyt c

The peroxidase activity of Cyt *c* was determined as described by Kim et al. [33]. Briefly, the peroxidase activity of Cyt *c* was measured by using a chromogen, 2.2′-azinobis-(2-ethylbenzthiazoline-6-sulfonate) (ABTS) [34]. The ABTS was dissolved in the ultrapure water and has a strong absorption at 340 nm. On oxidation, ABTS forms a stable cation radical, $ABTS^{+}$ which is conveniently followed at λ_{max} at 415 nm ($\varepsilon_{415=}3.6 \times 10^4$ M^{-1} cm^{-1}). The HEPES-Citrate solution (pH 7.4) was

used as the reaction medium. ABTS was diluted in the reaction medium. In parallel, Cyt *c* (20 μM) was incubated with AgNPs (20 μM), for different time points (t0 to 24h). The assay mixture contained of 100 μL of Cyt c-AgNPs mixture, 50 μM ABTS and 0.5 mM hydrogen peroxide (H_2O_2) in a total volume of 1 ml. The reaction was initiated by the addition of H_2O_2 and the increase in absorbance at 415 nm was measured by using a PerkinElmer UV/Visible spectrophotometer Lambda 365.

3. Result and discussion

3.1. AgNPs – Cyt c interactions

The hydrodynamic diameter of AgNPs, Cyt *c* alone, and in the mixture system, was first determined using DLS measurements made at two time points *t0* (*t0* denotes the shortest time to allow measurement immediately after mixing) and 24 h. The results demonstrated that AgNPs in HEPES-citrate buffer were monodisperse, with an average hydrodynamic diameter (d_h) of 21 ± 2 nm (Fig. 1A). Cyt *c* hydrodynamic diameters were found at 220 ± 6 nm revealing the aggregation of protein. Then the proteins were mixed with AgNPs. At the beginning (*t0*), 2 population appeared. One could correspond to the formation of AgNP-Cyt c complexes with $d_h = 25 \pm 3$ nm, the other to the aggregate protein (225 ± 8 nm) suggesting that a part of the large excess of protein used here did not react with the AgNP surface. After 24 h, the AgNP-Cyt c complexes (25 ± 3 nm) became the main population with an increase of volume percentage from 5% (*t0*) to 18%, demonstrating the "free protein" decrease in the mixture system, with a gradual enhancement of AgNP-Cyt c complex formation overtime.

Changes in SPR of AgNPs are a well-known sensitive indicator of the binding reaction to biomolecules [35]. As can be seen from Fig. 1B, the spectra of the AgNPs showed a characteristically intense SPR band at 398 nm. The native state of Cyt *c* (in HEPES citrate buffer at pH 7.4 in the absence of NPs) is characterized by the Soret peak observed at 420 nm and two absorption peaks at 520 and 550 nm which are the typical characteristics of the reduced state (Fe^{2+}) of the Cyt *c* (purple curve). Immediately mixing of Cyt *c* with AgNPs resulted in a significant increase of the signal intensity of SPR band at 411 nm. This SPR band overlapped Cyt *c* Soret peak and AgNPs SPR band could correspond to the formation of AgNP-Cyt c complexes. And two weak bands of Cyt *c* at 520 and 550 nm remained unchanged. After 24 h, the intensity of three peaks decreased suggesting Cyt *c* induced AgNP dissolution.

To further highlight the changes in the size of AgNPs and in the nature of the formed AgNPs-protein complexes, the AgNPs, and AgNPs + Cyt C mixture were then analyzed by TEM. TEM images of the AgNPs without proteins revealed similar size distributions at t0 and 24 h, with average diameters of 21 ± 5 nm and 19 ± 4 nm, respectively (Fig. 2). On the contrary, the TEM images of the mixture of AgNPs with Cyt *c* evolved differently over 24h. There was no significant change in their primary size with Cyt *c* at the beginning of the interaction (t0) (Fig. 2D). After 24h, TEM analysis of the AgNP-Cyt c mixture (Fig. 2E) revealed two size populations. One population corresponded the primary size distribution, and another had particles average diameter reduced (10.6 ± 3 nm), including some particles below 7 nm, resulting from nanoparticles dissolution leading to a release of Ag(I). This observation was coherent with the DLS and Uv–vis results (Fig. 1).

3.2. Binding thermodynamics of AgNPs with Cyt c

To get deeper insight into the mechanism of NPs-protein interaction, ITC experiments were also performed to obtain the information on energies exchanged during interaction such as binding affinity (association constant), interaction mechanisms (binding enthalpy, binding entropy and Gibbs free energy), and binding stoichiometry [36]. ITC experiments were carried out by titrating protein solutions into the sample cell containing AgNPs. As can be seen from the displacement enthalpy curve (Fig. 3), the evolution of displacement enthalpies evidenced the highest energy values at low coverage. It reflects the enthalpy of interaction between the protein molecule and the nanoparticle. The magnitude of the effect increases with increasing Cyt *c* molecules, evidencing that the Cyt *c* binding occurs on the surface of nanoparticles. It is worth noting that the nature of binding of Cyt *c* to AgNPs produces an exothermic effect around −60 kJ/mol which can be related to the contribution of electrostatic interactions between protein and AgNPs.

With the gradual addition of protein, the displacement enthalpy values decrease monotonically until a plateau around −10 kJ/mol. This behaviour may be due to the lateral interactions between adsorbed Cyt *c* onto AgNPs when the surface density became too high or a shielding effect when the monolayer is exceeded. By gradual injection of Cyt *c* into AgNPs solution, ΔH° reached a plateau indicating the saturation of surface coverage of AgNPs, with 4.36 protein molecules per nm^2 of AgNPs when ΔH° was -14.9 ± 3.3 kJ/mol. The affinity between the Cyt *c* and the surface reflected by the curvature of the thermogram at low recovery values is moderate.

Even if it is difficult to separate all the phenomena involved int adsorption process, it can be estimated that the main mechanism of adsorption is driven by enthalpy (high negative value of enthalpy change) with an unfavourable entropy change ($\Delta S^\circ < 0$). This positive entropy change is not surprising, because this behaviour is frequently encountered when conformation changes occur or when proteins lose degrees of freedom during the interaction process.

3.3. AgNPs effect on enzyme conformations

UV CD spectroscopy measurements were therefore carried out to better understand the influence of AgNPs on possible conformational change of Cyt *c*. The far-UV CD spectra of both free and adsorbed Cyt *c* indicated two main negative bands at about 209 nm and 222 nm, which

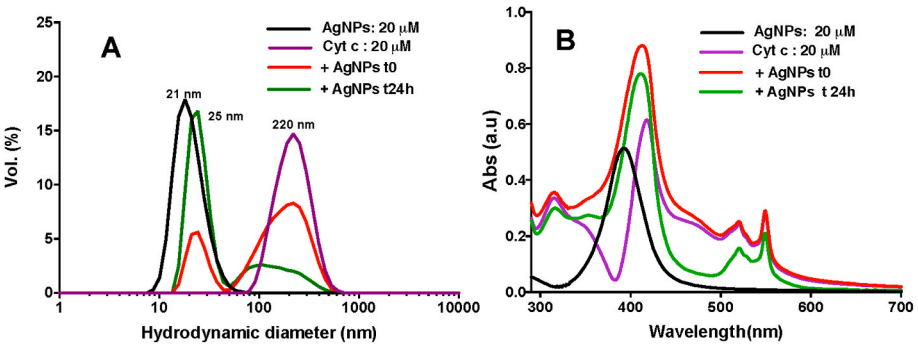

Fig. 1. Hydrodynamic diameter distribution (in % volume) in various suspensions (A); AgNPs (black), and AgNP-protein mixture UV–visible spectra of AgNPs with and without proteins, as a function of time (B). 20 μM AgNPs (black), 20 μM Cyt *c* (purple) and AgNP - protein mixture at t0 (red), and 24h (green).

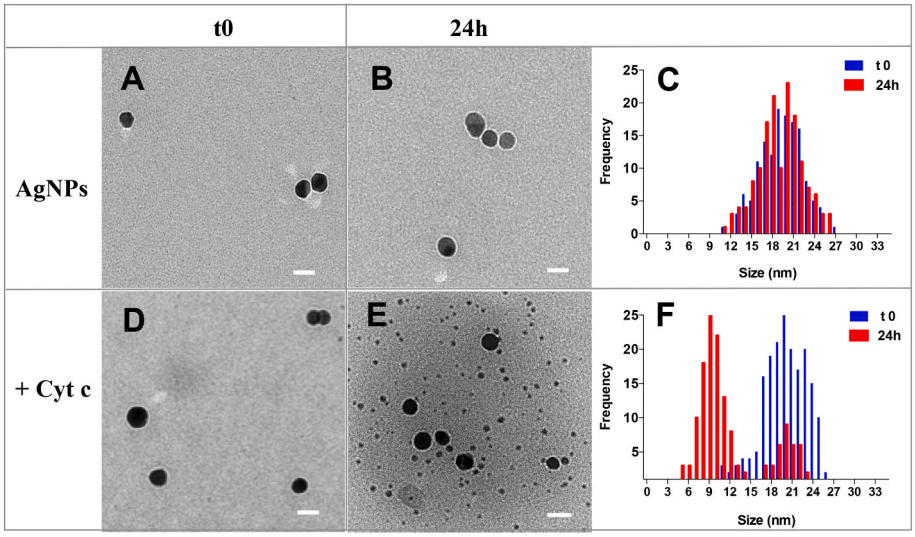

Fig. 2. TEM images of 20 μM AgNPs in different suspensions and at t0 (A) and 24 h incubation (B); C: size distribution analysis of the TEM images of the samples shown in A and B; the mixture of 20 μM AgNP and 20 μM Cyt *c* at t0 (D) and 24 h (E). F: size distribution analysis of the images of the samples presented in D and E. At least 100 particles were counted for each condition. The scale bar is 20 nm.

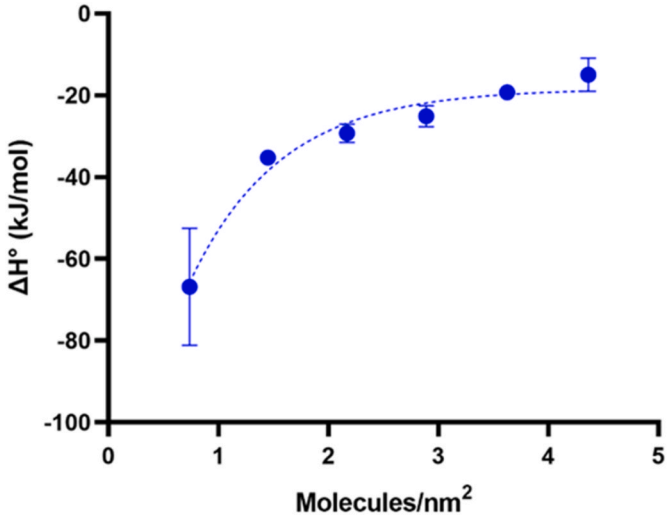

Fig. 3. Displacement enthalpy change versus surface density of CytC into the suspension of AgNPs.

are characteristic of α-helical secondary structure of proteins (Fig. 4A). With AgNPs, the intensity of such bands increased with interaction time (Fig. 4A). These results indicate that the secondary structure of Cyt *c* has been altered.

For the near-UV CD measurements, the Cyt *c* concentration used for far-UV CD was too low to be detectable. So, we have increased the Cyt *c* concentration but kept the molar ratio Cyt *c*: AgNPs to 1:1 as used in other experiments. As shown in Fig. 4B, the CD spectra in the Soret region (380–450 nm) arise from interaction of the heme electronic transitions with those of nearby aromatic amino acid residues, which can provide information on protein structural integrity in the vicinity of the heme group [22]. Specifically, the positive band at 407 nm increases and the negative band at 418 nm decreases in the presence of AgNPs over time. Therefore, these results highlighted the fact that AgNPs-Cyt c interactions exist and modify the Cyt *c* secondary structural elements. The binding of Cyt *c* onto AgNPs results in a remarkable structural perturbation around the active site heme.

Fluorescence spectroscopy is commonly used as a sensitive method for determining the modes of interaction between a protein and a ligand, including the accessibility and mechanism of fluorophore quenching [37]. Intrinsic fluorescence from Trp and Tyr residues are sensitive internal probes of protein tertiary structure due to the high sensitivity of fluorescence signals to changes in their microenvironment [38]. Fig. 5 is the fluorescence spectra of Cyt *c* with the concentration of AgNPs from 0 to 60 μM. It can be seen that with the gradual addition of AgNPs, Cyt *c* fluorescence emission was quenched, as shown by the progressive reduction in fluorescence intensity at 350 nm. The decrease of fluorescence intensity of Cyt *c* reached the maximum and became stable for the AgNPs concentration higher than 40 μM. This result indicates that Cyt *c* could bind to the surface of AgNPs and that this phenomenon modifies the tertiary structure of Cyt *c*.

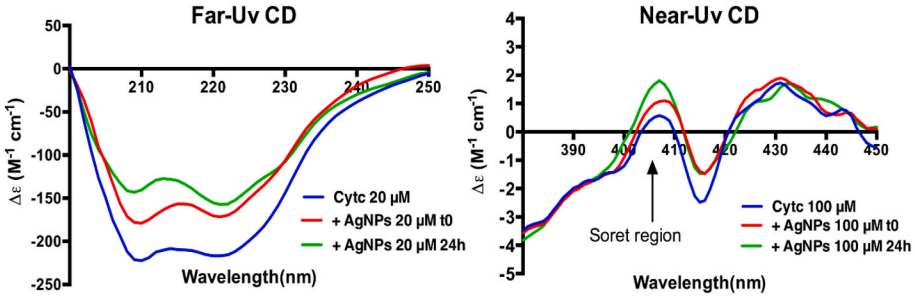

Fig. 4. Far -UV CD (A) and Soret CD spectra (B) of free Cyt *c* and after contact with AgNPs at the beginning and 24h incubation. The concentration of the Cyt *c* and AgNPs was fixed at 20 μM and 100 μM with protein/AgNP mole ratio of 1:1.

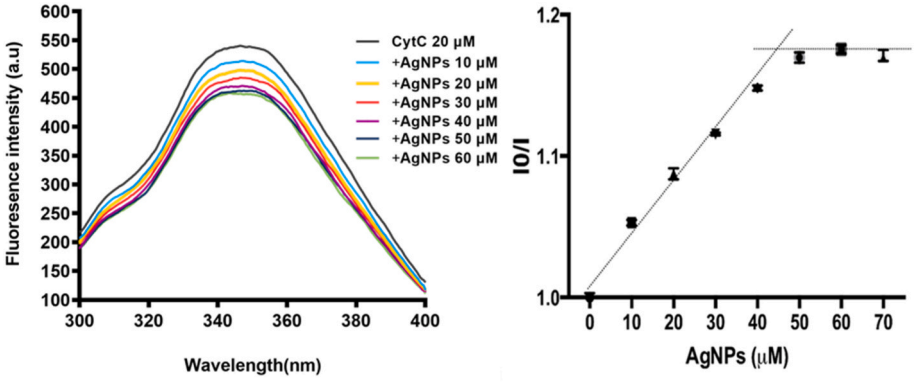

Fig. 5. Evolutions of fluorescence spectra of Cyt *c* with increasing concentration of AgNPs (A). The concentration of the Cyt *c* was kept at 20 μM. The emission spectrum of AgNPs alone was negligible at 280 nm excitation wavelength. *I0/I* varied linearly with the addition of NPs and could be expressed as $1 + k_{SV}$ [NPs], in which k_{SV} is the Stern–Volmer constant.

To gain a better understanding of the quenching mechanism, we analyzed the fluorescence intensity data using the standard Stern-Volmer equation. The quenching data was presented in Fig. 5B and are characterized as two linear regions with distinct slopes. The first has been attributed to the specific interaction resulting in a predominant static quenching. The AgNPs-Cyt c complex was formed and prevented the emission of the fluorescence in this process. Whereas the second slope could be due to saturation of the complexation sites. These results point to the formation of complexes between AgNPs and proteins. The AgNP-protein binding process results in conformational changes in Cyt *c*, as UV–vis absorption and CD spectroscopy suggest, leading to the accessibility of initially protected fluorescent residues for AgNPs. Enzyme structural changes can lead to loss of biological function, because there is a significant correlation exists between conformational folding and functional specificity [39].

3.4. *Influence of AgNPs on enzyme activities*

To test whether the interaction between Cyt *c* and AgNPs resulted in the perturbation of the Cyt *c* biological function, the peroxidase-like activity of protein was probed by monitoring the oxidation of ABTS by H_2O_2 in the presence of AgNPs. The peroxidase-like activity of Cyt *c* has been shown to be critical for the release of this and other proteins from mitochondria early in apoptosis [40]. Like other peroxidase, the activity of Cyt *c* follows a mechanism where H_2O_2 reacts with the Fe(III) resting state to produce "compound I″, with a Fe(IV)═O heme and an adjacent radical. The reaction of the newly formed radicals with O_2 then yields stable oxidation products [41–43]. As shown in Fig. 6, AgNPs activate Cyt *c* toward the oxidation of ABTS, a significant enzyme activity was measured in the presence of AgNP from 30 min incubation. And then the peroxidase-like activity of Cyt *c* increased slowly, with a similar trend of enzyme activity activation of 127.4 ± 1.7% and 134.3 ± 5.8% after 2h and 24 h. These changes are in accordance with AgNPs induced conformational changes of Cyt *c*, in which the tertiary structure of Cyt *c* in the presence of AgNPs was less compact relative to native protein, as shown by a decrease in fluorescence intensity (Fig. 5). Moreover, the results depicted in Fig. 4B indicate that the heme environment is influenced with an increase in near CD intensities for aromatic residues and heme by adsorption of Cyt *c* onto AgNPs, and that more significant perturbation of the heme environment is overtime.

This observation is in agreement with the existing literature, which showing that Cyt *c* activity can be increased after interacting with silica NPs [22,23] and iron NPs [44]. These studies indicated that the protein conformational changes after interaction with NPs could considerably increase the access of H_2O_2 to the heme group. Hence, the change in the environment of heme in the presence of AgNPs in our study may lead to a more access site for H_2O_2 molecules and resulted in the activation of the peroxidase-like mechanism of Cyt *c*.

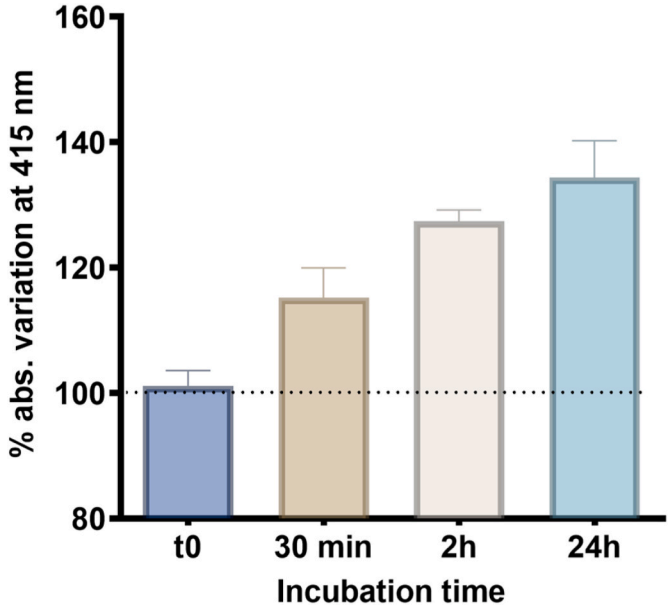

Fig. 6. Changes in Cyt *c* activity over 24 h of incubation in the presence of AgNPs. AgNPs does not show any kind of activity like Cyt *c* (data not shown).

4. Conclusion

The present work explored structural and conformational changes to assess the interaction of AgNPs with Cyt *c* in terms of the NPs stability, proteins conformation and function by using a combination of multiple spectral, imaging and thermodynamic methods. It was found that Cyt *c* interacted with AgNPs and formed surface complexes. The thermodynamic parameters (binding enthalpy) demonstrated that the binding of Cyt *c* to AgNPs was a spontaneous reaction and electrostatic forces of attraction played a major role in the interaction. The interaction between Cyt *c* and the AgNP surface promoted conformational changes in the protein with time effect evidencing by CD and fluorescence spectroscopy experiments, that ultimately affect the heme microenvironment. And this AgNPs-Cyt c complex formation also induced the dissolution of AgNPs. The dissolving Ag together with AgNPs altered the peroxidase-like activity of Cyt *c*. This research provides a basis of understanding how the functional properties of antioxidant protein may affect the stability of nanoparticles and, vice versa, how the NPs could affect the conformation and reactivity of protein. These results also

extend our knowledge in the biochemical reactivity of AgNPs with proteins and could help establish the *in vivo* fate of AgNPs. Further studies are needed to reveal the occurrence and influence of alternative conformations Cyt *c* in the processes associated with changes in mitochondrial and cellular redox homeostasis.

Credit author statement

WL: Conceptualization, Methodology, Formal analysis, Investigation, Writing - original draft. Funding acquisition. DBL: Methodology, Investigation, Writing – review & editing. FC: Methodology, Investigation, Writing – review & editing. VIS: Funding acquisition, Writing – review & editing.

Declaration of competing interest

The authors declare that they have no known competing financial interests or personal relationships that could have appeared to influence the work reported in this paper.

Data availability

Data will be made available on request.

Acknowledgment

Financial support was provided by the University of Geneva and Swiss National Science Foundation (grant number 197322).

Appendix A. Supplementary data

References

[1] Z. Zhou, M. Vázquez-González, I. Willner, Stimuli-responsive metal–organic framework nanoparticles for controlled drug delivery and medical applications, Chem. Soc. Rev. 50 (2021) 4541–4563.
[2] P. Kowalczyk, M. Szymczak, M. Maciejewska, Ł. Laskowski, M. Laskowska, R. Ostaszewski, G. Skiba, I. Franiak-Pietryga, All that glitters is not silver—a new look at microbiological and medical applications of silver nanoparticles, Int. J. Mol. Sci. 22 (2021) 854.
[3] N. Faisal, K. Kumar, Polymer and metal nanocomposites in biomedical applications, Biointerface Research in Applied Chemistry 7 (2017) 2286–2294.
[4] A.-C. Burduşel, O. Gherasim, A.M. Grumezescu, L. Mogoantă, A. Ficai, E. Andronescu, Biomedical applications of silver nanoparticles: an up-to-date overview, Nanomaterials 8 (2018) 681.
[5] L. Hannibal, F. Tomasina, D.A. Capdevila, V. Demicheli, V. Tortora, D. Alvarez-Paggi, R. Jemmerson, D.H. Murgida, R. Radi, Alternative conformations of cytochrome c: structure, function, and detection, Biochemistry 55 (2016) 407–428.
[6] J.M. Stevens, Cytochrome c as an experimental model protein, Metallomics 3 (2011) 319–322.
[7] H. Bayir, B. Fadeel, M. Palladino, E. Witasp, I. Kurnikov, Y. Tyurina, V. Tyurin, A. Amoscato, J. Jiang, P. Kochanek, Apoptotic interactions of cytochrome c: redox flirting with anionic phospholipids within and outside of mitochondria, Biochimica et Biophysica Acta (BBA)-Bioenergetics 1757 (2006) 648–659.
[8] R.R.R. Sardari, S.R. Zarchi, S. Hajihosseini, Z. Aghili, R. Rasoolzadeh, S. Imani, H. Borna, A.M. Zand, A. Nejadmoghadam, M. Ghalavand, Identification of an independent measurement method for denaturation studies of cytochrome C, Int. J. Electrochem. Sci. 8 (2013) 11578–11587.
[9] R. Krieg, K. Halbhuber, Recent advances in catalytic peroxidase histochemistry, Cell. Mol. Biol. 49 (2003) 547–563.
[10] R.A. Scott, A.G. Mauk, Cytochrome C: a Multidisciplinary Approach, Univ Science Books, 1996.
[11] V.E. Kagan, V.A. Tyurin, J. Jiang, Y.Y. Tyurina, V.B. Ritov, A.A. Amoscato, A. N. Osipov, N.A. Belikova, A.A. Kapralov, V. Kini, Cytochrome c acts as a cardiolipin oxygenase required for release of proapoptotic factors, Nat. Chem. Biol. 1 (2005) 223–232.
[12] K.L. Bren, E.L. Raven, Locked and loaded for apoptosis, Science 356 (2017) 1236, 1236.
[13] M.W. Mara, R.G. Hadt, M.E. Reinhard, T. Kroll, H. Lim, R.W. Hartsock, R. Alonso-Mori, M. Chollet, J.M. Glownia, S. Nelson, Metalloprotein entatic control of ligand-metal bonds quantified by ultrafast x-ray spectroscopy, Science 356 (2017) 1276–1280.
[14] K. Peynshaert, B.B. Manshian, F. Joris, K. Braeckmans, S.C. De Smedt, J. Demeester, S.J. Soenen, Exploiting intrinsic nanoparticle toxicity: the pros and cons of nanoparticle-induced autophagy in biomedical research, Chem. Rev. 114 (2014) 7581–7609.
[15] M.-E. Aubin-Tam, K. Hamad-Schifferli, Gold nanoparticle− cytochrome C complexes: the effect of nanoparticle ligand charge on protein structure, Langmuir 21 (2005) 12080–12084.
[16] X. Jiang, J. Jiang, Y. Jin, E. Wang, S. Dong, Effect of colloidal gold size on the conformational changes of adsorbed cytochrome c: probing by circular dichroism, UV− Visible, and Infrared Spectroscopy, Biomacromolecules 6 (2005) 46–53.
[17] J.M. Wallace, R.M. Stroud, J.J. Pietron, J.W. Long, D.R. Rolison, The effect of particle size and protein content on nanoparticle-gold-nucleated cytochrome c superstructures encapsulated in silica nanoarchitectures, J. Non-Cryst. Solids 350 (2004) 31–38.
[18] H. Bayraktar, C.-C. You, V.M. Rotello, M.J. Knapp, Facial control of nanoparticle binding to cytochrome c, J. Am. Chem. Soc. 129 (2007) 2732–2733.
[19] M. Simsikova, M. Antalik, Interaction of cytochrome c with zinc oxide nanoparticles, Colloids Surf. B Biointerfaces 103 (2013) 630–634.
[20] M. Simsikova, M. Antalik, M. Kanuchova, J. Skvarla, Cytochrome c conjugated to ZnO-MAA nanoparticles: the study of interaction and influence on protein structure, Int. J. Biol. Macromol. 59 (2013) 235–241.
[21] L. Wang, E. Wang, Direct electron transfer between cytochrome c and a gold nanoparticles modified electrode, Electrochem. Commun. 6 (2004) 49–54.
[22] W. Shang, J.H. Nuffer, V.A. Muniz-Papandrea, W. Colon, R.W. Siegel, J.S. Dordick, Cytochrome C on silica nanoparticles: influence of nanoparticle size on protein structure, stability, and activity, Small 5 (2009) 470–476.
[23] L. Tarpani, F. Bellezza, P. Sassi, M. Gambucci, A. Cipiciani, L. Latterini, New insights into the effects of surface functionalization on the peroxidase activity of cytochrome c adsorbed on silica nanoparticles, J. Phys. Chem. B 123 (2019) 2567–2575.
[24] A. Mukhopadhyay, N. Joshi, K. Chattopadhyay, G. De, A facile synthesis of PEG-coated magnetite (Fe3O4) nanoparticles and their prevention of the reduction of cytochrome c, ACS Appl. Mater. Interfaces 4 (2012) 142–149.
[25] S.T. Kim, Y.-J. Lee, Y.-S. Hwang, S. Lee, Study on aggregation behavior of Cytochrome C–conjugated silver nanoparticles using asymmetrical flow field-flow fractionation, Talanta 132 (2015) 939–944.
[26] W. Liu, I.A.M. Worms, S. Vera, Interaction of silver nanoparticles with key antioxydant enzymes, Environ. Sci. Nano 7 (2020) 1507–1517.
[27] W. Liu, I.A.M. Worms, N. Herlin-Boime, D. Truffier-Boutry, I. Michaud-Soret, E. Mintz, C. Vidaud, F. Rollin-Genetet, Interaction of silver nanoparticles with metallothionein and ceruloplasmin: impact on metal substitution by Ag(i), corona formation and enzymatic activity, Nanoscale 9 (2017) 6581–6594.
[28] A. Käkinen, F. Ding, P. Chen, M. Mortimer, A. Kahru, P.C. Ke, Interaction of firefly luciferase and silver nanoparticles and its impact on enzyme activity, Nanotechnology 24 (2013), 345101.
[29] D.N. Freitas, A.J. Martinolich, Z.N. Amaris, K.E. Wheeler, Beyond the passive interactions at the nano-bio interface: evidence of Cu metalloprotein-driven oxidative dissolution of silver nanoparticles, J. Nanobiotechnol. 14 (2016) 1–6.
[30] A.J. Martinolich, G. Park, M.Y. Nakamoto, R.E. Gate, K.E. Wheeler, Structural and functional effects of Cu metalloprotein-driven silver nanoparticle dissolution, Environ. Sci. Technol. 46 (2012) 6355–6362.
[31] L. Gebicka, Peroxidase-like activity of cytochrome c in the presence of anionic surfactants, Res. Chem. Intermed. 27 (2001) 717–723.
[32] J.M. Gorham, A.B. Rohlfing, K.A. Lippa, R.I. MacCuspie, A. Hemmati, R. D. Holbrook, Storage Wars: how citrate-capped silver nanoparticle suspensions are affected by not-so-trivial decisions, J. Nanopar. Res. 16 (2014) 1–14.
[33] N.-H. Kim, M.-S. Jeong, S.-Y. Choi, J.-H. Kang, Peroxidase activity of cytochrome c, Bull. Kor. Chem. Soc. 25 (2004) 1889–1892.
[34] R. Radi, L. Thomson, H. Rubbo, E. Prodanov, Cytochrome c-catalyzed oxidation of organic molecules by hydrogen peroxide, Arch. Biochem. Biophys. 288 (1991) 112–117.
[35] V. Banerjee, K. Das, Interaction of silver nanoparticles with proteins: a characteristic protein concentration dependent profile of SPR signal, Colloids Surf. B Biointerfaces 111 (2013) 71–79.
[36] D. Prozeller, S. Morsbach, K. Landfester, Isothermal titration calorimetry as a complementary method for investigating nanoparticle-protein interactions, Nanoscale 11 (2019) 19265–19273.
[37] R. Huang, R.P. Carney, K. Ikuma, F. Stellacci, B.L. Lau, Effects of surface compositional and structural heterogeneity on nanoparticle–protein interactions: different protein configurations, ACS Nano 8 (2014) 5402–5412.
[38] F. Bellezza, A. Cipiciani, L. Latterini, T. Posati, P. Sassi, Structure and catalytic behavior of myoglobin adsorbed onto nanosized hydrotalcites, Langmuir 25 (2009) 10918–10924.
[39] K.A. Dill, J.L. MacCallum, The protein-folding problem, 50 years on, Science 338 (2012) 1042–1046.
[40] P. Ascenzi, M. Coletta, M.T. Wilson, L. Fiorucci, M. Marino, F. Polticelli, F. Sinibaldi, R. Santucci, Cardiolipin–cytochrome c complex: switching cytochrome c from an electron-transfer shuttle to a myoglobin-and a peroxidase-like heme-protein, IUBMB Life 67 (2015) 98–109.
[41] A.N. Volkov, P. Nicholls, J.A. Worrall, The complex of cytochrome c and cytochrome c peroxidase: the end of the road? Biochimica et Biophysica Acta (BBA)-Bioenergetics 1807 (2011) 1482–1503.

[42] G. Xu, M.R. Chance, Hydroxyl radical-mediated modification of proteins as probes for structural proteomics, Chem. Rev. 107 (2007) 3514–3543.
[43] V. Yin, G.S. Shaw, L. Konermann, Cytochrome c as a peroxidase: activation of the precatalytic native state by H2O2-induced covalent modifications, J. Am. Chem. Soc. 139 (2017) 15701–15709.
[44] V. Jafari Azad, S. Kasravi, H. Alizadeh Zeinabad, M. Memar Bashi Aval, A. A. Saboury, A. Rahimi, M. Falahati, Probing the conformational changes and peroxidase-like activity of cytochrome c upon interaction with iron nanoparticles, J. Biomol. Struct. Dyn. 35 (2017) 2565–2577.